

Structure determination of two intercalated compounds $\text{VOPO}_4 \cdot (\text{CH}_2)_4\text{O}$ and $\text{VOPO}_4 \cdot \text{OH} - (\text{CH}_2)_2 - \text{O} - (\text{CH}_2)_2 - \text{OH}$; synchrotron powder diffraction and molecular modelling

Kees Goubitz,^{a*} Pavla
Čapková,^{a,b} Klára Melánová,^b
Wim Molleman^a and Henk
Schenk^a

^aLaboratory for Crystallography, Institute for Molecular Chemistry (IMC), Universiteit van Amsterdam, Nieuwe Achtergracht 166, 1018 WV Amsterdam, The Netherlands, and

^bDepartment of Chemical Physics and Optics, Faculty of Mathematics and Physics, Charles University Prague, Ke Karlovu 3, 12116 Prague 2, Czech Republic

Correspondence e-mail: fz@crys.chem.uva.nl

Received 7 July 2000

Accepted 27 October 2000

The crystal structures of two intercalated compounds have been determined using a combination of synchrotron powder diffraction and molecular mechanics simulations: (1) vanadyl phosphate intercalated with tetrahydrofuran, $\text{VOPO}_4 \cdot (\text{CH}_2)_4\text{O}$, and (2) vanadyl phosphate intercalated with diethylene glycol, $\text{VOPO}_4 \cdot \text{HO}(\text{CH}_2)_2\text{O}(\text{CH}_2)_2\text{OH}$. Both intercalates preserve the tetragonal space group $P4/n$, as found in the host structure $\text{VOPO}_4 \cdot 2\text{H}_2\text{O}$. (1): $a = 6.208$, $c = 8.930$ Å, $Z = 2$, $D_x = 2.51$ g cm⁻³; (2): $a = 6.223$, $c = 11.417$ Å, $Z = 2$, $D_x = 2.66$ g cm⁻³. Both intercalates exhibit the same type of orientational disorder in the arrangement of guest molecules, as observed in the same host compound intercalated with water. These two intercalates also exhibit, rather surprisingly, perfect ordering in layer stacking without the displacement disorder, characteristic of many intercalated layered structures. Thanks to this regularity in the arrangement of guests and layers, synchrotron powder diffraction could be used in the present structure determination. The present results also enabled the analysis of the effect of geometrical parameters characterizing the mutual host–guest complementarity and the effect of host–guest and guest–guest interaction on the crystal packing of intercalates.

1. Introduction

Intercalation of inorganic layered host compounds with organic species results in a hybrid organic/inorganic structure, where the two-dimensional supramolecular system of organic guest molecules in the interlayer space of the host structure exhibits changes in electronic properties owing to the crystal field of the host layers. This method of modification of the electronic properties is used in the development of new materials with interesting photofunctions for optoelectronic devices (Ogawa & Kuroda, 1995). The layered structure of vanadyl phosphate represents a very suitable host compound for intercalation of polar organic molecules. The host layers possess strong active sites for anchoring the guest molecules. The presence of strong active sites is the important factor which gives rise to a stable intercalated structure (Clearfield, 1982), and which also makes vanadyl phosphate a very convenient host compound for basic investigation of the intercalation behaviour of organic guest molecules in an inorganic host. In addition, great interest in intercalates based on vanadyl and zirconium phosphates arises from their remarkable physico-chemical properties (see Clearfield, 1982; Costantino, 1981).

Crystal packing of intercalates is the result of a joint effect of several factors characterizing the mutual complementarity

of the host structure and guest species such as: (1) the relationship between the structural parameters and symmetry of the host layer and guest species, and (2) the relationship between the host–guest and guest–guest interaction energy. Structural analysis of intercalates exhibits certain specific features arising from the method of preparation. As the intercalation is in fact the positioning of known molecules into a known crystal structure, the main task in structure determination of intercalates is to find the arrangement of guest molecules in the interlayer space, including possible conformational changes, and to determine the precise method of layer stacking. As the host–guest complementarity is not usually completely perfect, the structures of intercalates may possess a certain degree of disorder, which may hamper the structure determination based on powder diffraction data only. In such a case a molecular-mechanics simulation is a very useful complementary tool to investigate the details of interlayer crystal packing.

In this present work we used the combination of high-resolution synchrotron powder diffraction with molecular-mechanics simulations in the *Cerius*² (Molecular Simulations Inc., 1995) modelling environment to determine the structures of vanadyl phosphate intercalated with tetrahydrofuran (thf) and diethylene glycol (DEG) (see Fig. 1). The host structure of vanadyl phosphate dihydrate $\text{VOPO}_4 \cdot 2\text{H}_2\text{O}$ has been determined by Tietze (1981) from single-crystal diffraction data as tetragonal, space group $P4/nmm$ with $a = 6.202$, $c = 7.41$ Å and $Z = 2$. Tachez *et al.* (1982) presented the results of structure refinement of the deuterated compound $\text{VOPO}_4 \cdot 2\text{D}_2\text{O}$ based on neutron powder diffraction data: space group $P4/n$, $a = 6.2154$, $c = 7.4029$ Å and $Z = 2$. The host structure of vanadyl phosphate consists of infinite sheets of distorted VO_6 octahedra and PO_4 tetrahedra linked by shared O atoms (see Fig. 2*a*). Shared water molecules link these sheets together, creating a regular network of hydrogen bridges in the interlayer space (Fig. 2*b*). As one can see from Fig. 2*b*, there are two differently bonded water molecules in the interlayer space: one water molecule is attached with its oxygen to vanadium to complete the VO_6 octahedron and the second one is hydrogen bonded to PO_4 O atoms and to the first water molecule. Since both water molecules occur in two symmetry-equivalent orientations with an occupancy of 0.5, two equivalent networks of hydrogen bonds occur in the interlayer space corresponding to two orientations of water molecules. (For a more detailed description of the host structure see

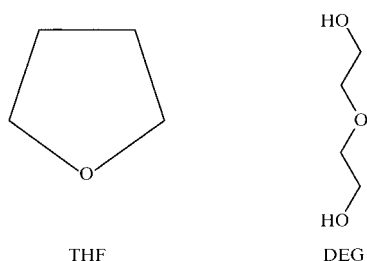


Figure 1
Intercalated molecules tetrahydrofuran (thf) and diethylene glycol (DEG).

Tachez *et al.*, 1982.) This type of interlayer arrangement of water molecules with two possible orientations can also occur in the arrangement of other intercalated species.

Interlayer water in the host structure $\text{VOPO}_4 \cdot 2\text{H}_2\text{O}$ is very weakly bonded and can be easily replaced by organic molecules. Then the intercalated molecules have to supply an O atom to complete the VO_6 octahedra. This implies that the empty apex of the VO_6 octahedron represents a strong active site for the anchoring of the organic molecule *via* a suitable O atom.

2. Experimental

2.1. Sample preparation

Vanadyl phosphate dihydrate was obtained by boiling vanadium pentoxide in diluted phosphoric acid under reflux for 14 h (Ladwig, 1965). The resulting yellow solid was filtered and washed with distilled water, and then dried at room temperature in ambient air. Direct intercalation of tetrahydrofuran (thf) and diethylene glycol (DEG) into anhydrous vanadyl phosphate or the dihydrate of vanadyl phosphate was not successful. Both intercalation compounds thf- VOPO_4 and DEG- VOPO_4 were obtained by a re-intercalation reaction of propanol-intercalated vanadyl phosphate. This latter precursor was prepared by heating a suspension of $\text{VOPO}_4 \cdot 2\text{H}_2\text{O}$ in dry propanol in a microwave field for 1 min (Beneš *et al.*, 1997).

In the case of thf- VOPO_4 , 1 g of solid $\text{VOPO}_4 \cdot 2\text{C}_3\text{H}_7\text{OH}$ was suspended in 30 ml of liquid thf and stirred for 1 d at room temperature. The solid product was filtered and dried in

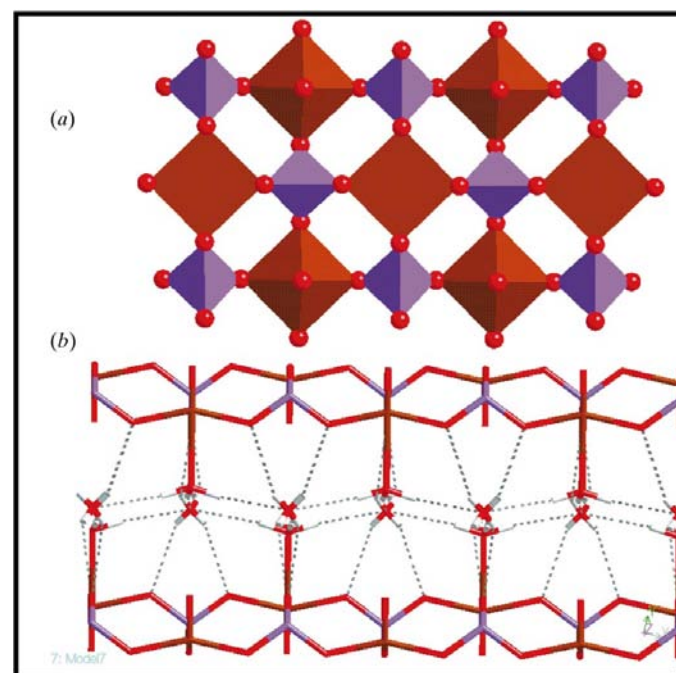


Figure 2
The host structure $\text{VOPO}_4 \cdot 2\text{H}_2\text{O}$: (a) view of the host layer VOPO_4 and (b) side view into the interlayer arrangement of water molecules.

nitrogen (Beneš *et al.*, 1997). The content of thf in the intercalate was determined by thermogravimetry and elemental analysis (C, H). For $\text{VOPO}_4(\text{CH}_2)_4\text{O}$ we obtained: C 20.61, H 3.39% (experimental) and C 20.53, H 3.45% (calculated).

In the case of DEG-VOPO_4 , 1 g of $\text{VOPO}_4 \cdot 2\text{C}_3\text{H}_7\text{OH}$ was suspended in 50 ml of liquid DEG and stirred for 4 d at 313 K. The solid product was filtered and washed with acetonitrile and stored over P_2O_5 (Melánová *et al.*, 1999). The content of DEG in the intercalate, determined by thermogravimetry and elemental analysis, was: C 17.85, H 3.80% (experimental) and C 17.92, H 3.76% (calculated).

2.2. High-resolution synchrotron powder diffraction measurements

X-ray powder diffraction patterns were measured at the high-resolution powder diffractometer BM16 (Fitch, 1996) at the European Synchrotron Radiation Facility (ESRF, Grenoble, France) with $\lambda = 0.445348 \text{ \AA}$. This wavelength was calibrated by measuring 11 peaks from *NIST* Si standard 640b (lattice parameter certified as 3.569094 \AA). These peaks were fitted with a pseudo-Voigt profile function to obtain peak positions, accounting for asymmetry using the Finger–Cox–Jephcoat correction, and then fitting the wavelength and instrumental zero-point to these positions *via* least-squares methods. For data collection a capillary with a diameter of 1.5 mm was filled with powder and rotated during exposure. Continuous scans were made from 0.0 to 44.0° in 2θ , with $0.5^\circ 2\theta \text{ min}^{-1}$ and a sampling time of 50 ms. Rather than measuring every 2θ range at the same time, the higher-angle regions of the patterns were measured several times in order to mimic a single-crystal measurement as much as possible, *i.e.* we tried to

give every reflection the same data collection time. After data collection the scans were binned at $0.005^\circ 2\theta$ and scaled.

3. Modelling strategy, structure solution and refinement

3.1. Vanadyl phosphate intercalated with thf

Full-pattern decomposition (FPD) in space group $P1$ with a split-type pseudo-Voigt peak profile function (*MRIA*: Zlokazov & Chernyshev, 1992) converged to $R_p = 0.123$. Importing the atomic positions of the VOPO_4 layer and performing a grid search with the program *MRIA* (Chernyshev & Schenk, 1998), using 70 low-angle reflections, yielded the thf O atom (O_{thf}) bonded to V at a distance of 2.41 \AA . A continued grid search resulted in four C atoms at 1.5 \AA from O_{thf} forming an almost perfect rectangle, thus suggesting the thf moiety to be positioned in such a way that two thf rings share O_{thf} and, consequently, that the C atoms must have an occupancy of 0.5 in space group $P4/n$.

This rough model obtained from diffraction data was completed by insertion of the rest of the thf molecule and used as the initial model for molecular-mechanics simulations in *Cerius*². The charges in *Cerius*² were calculated using the Qeq method (charge-equilibrium approach, see Rappe & Goddard, 1991). To describe the potential energy we used the Burchart Universal force field, which was designed for modelling of sorption of organic molecules into zeolites and aluminophosphates. It is in fact a combination of two force fields: the Universal force field (Rappé *et al.*, 1992) and the Burchart force field (Burchart, 1992). Energy minimization has been carried out under the following constraints: fixed

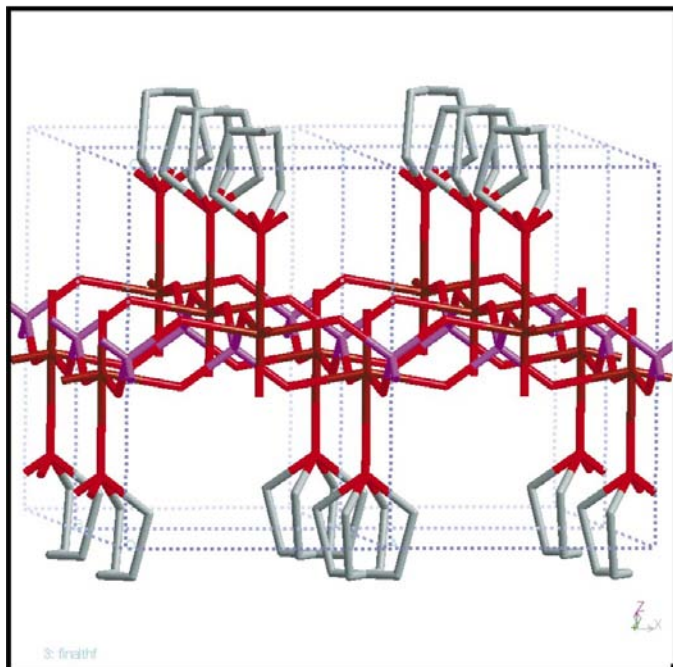


Figure 3
The anchoring of thf molecules to the VOPO_4 layers (four unit cells, H atoms are omitted).

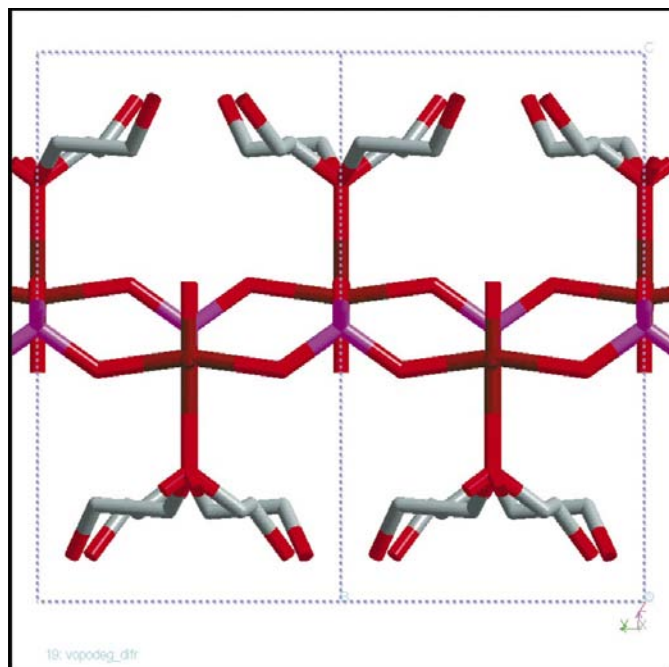


Figure 4
The anchoring of DEG molecules to the VOPO_4 layers (two unit cells, atoms omitted).

unit-cell parameters as obtained from the diffraction data, fixed atomic positions in the VOPO_4 layer and fixed position of the thf oxygen O_{thf} .

As a result of energy minimization, we obtained two models with the same crystal energy but with different orientations of the thf molecule (see Fig. 3). Rotation of thf molecules around the $\text{V}-\text{O}_{\text{thf}}$ axis showed that the two thf positions shown in Fig. 3 correspond to the minimum of the total sublimation energy, which is equal for both orientations. The minimized model in $P1$ was examined and it was possible to describe the model in the (correct) space group $P4/n$ (all C and H atoms have occupancy factors of 0.5). This last model has been taken as the starting model in the bond-restrained Rietveld refinement (RR) with the program *MRIA*. The bonds were restrained to the values obtained from the molecular-mechanics calculations with e.s.d.'s of 1% of these values. The restraints were gradually relaxed but not released. A split-type pseudo-Voigt peak profile function was used and asymmetry and anisotropic line broadening was taken into account. Preferred orientation was taken into account using symmetrized-harmonics expansion (Ahtee *et al.*, 1989; Järvinen, 1993).

3.2. Vanadyl phosphate intercalated with DEG

Full-pattern decomposition (FPD) converged to $R_p = 0.171$. In the case of $\text{DEG}-\text{VOPO}_4$ the rough structure model obtained from the diffraction data contained only the structure of the VOPO_4 layer and with good accuracy the position of the O atom bonded to V with a $\text{V}-\text{O} \approx 2.4 \text{ \AA}$. In this case the experimental electron density map in the interlayer space was much smoother than in $\text{thf}-\text{VOPO}_4$. It was also not clear from the electron density maps if the O atom attached to vanadium was the central one or the terminal O(H) oxygen of the DEG molecule. Therefore, a series of possible initial models was prepared for energy minimization in *Cerius*². All these models had different positions and orientations of the DEG molecule with respect to the VOPO_4 layers, thus having

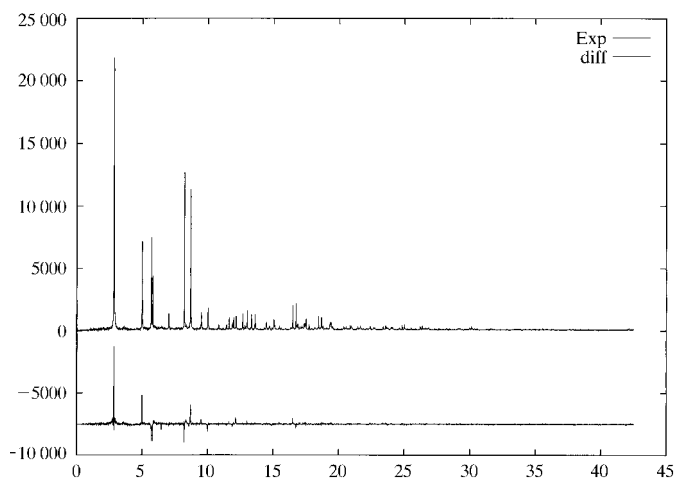


Figure 5
Bond-restrained Rietveld refinement of $\text{thf}-\text{VOPO}_4$. The upper curve illustrates the observed data, while the lower curve is the difference between observed and calculated data.

Table 1

Details of the bond-restrained Rietveld refinement.

The numbers in parentheses are after full pattern decomposition and RR without preferred orientation, respectively.

	$\text{VOPO}_4\cdot\text{thf}$	$\text{VOPO}_4\cdot\text{DEG}$
2θ region ($^\circ$)	0.005–42.500	0.005–42.500
No. of data points	8500	8500
No. of reflections	825	1060
No. of restraints	55	66
No. of variables		
Lattice	2	2
Positional	12	15
Thermal	5	4
Texture	5	5
Profile	13	13
Background	12	12
GoF	4.0 (4.4)	7.2 (6.7)
R_p	0.132 (0.123; 0.144)	0.199 (0.171; 0.237)
	$\text{VOPO}_4\cdot\text{thf}$	$\text{VOPO}_4\cdot\text{DEG}$
wR	0.145 (0.156; 0.156)	0.228 (0.209; 0.267)

either a terminal O(H) or the central O atom bonded to vanadium. The strategy of energy minimization was the same as in the case of $\text{thf}-\text{VOPO}_4$: application of the Burchart Universal force field, fixed unit-cell parameters obtained from diffraction data, fixed atomic positions in the VOPO_4 layer and a fixed O atom bonded to vanadium. The results of the molecular-mechanics simulations showed that the best model with a minimum of the crystal energy was obtained for the DEG molecule attached to the VOPO_4 layer *via* the anchoring of its central O atom (see Fig. 4). Molecular modelling also revealed that, as in the case of $\text{thf}-\text{VOPO}_4$, two possible orientations of the DEG molecule with the same crystal energy were possible (see Fig. 4). As with the compound $\text{thf}-\text{VOPO}_4$, all calculations were performed in space group $P1$ and from the resulting model the symmetry was re-established as $P4/n$ with, consequently, four $(\text{CH}_2)_2\text{OH}$ groups with occupancy 0.5 connected to the central O of DEG. This model was used as a starting model for the bond-restrained RR. The results of the FPD and RR are listed in Table 1. The atomic coordinates of $\text{thf}-\text{VOPO}_4$ and $\text{DEG}-\text{VOPO}_4$ have been deposited.¹ Plots of the observed X-ray diffraction patterns and difference plots after RR of both compounds are depicted in Figs. 5 and 6.

4. Results and discussion

4.1. Structure of $\text{thf}-\text{VOPO}_4$

The structure of vanadyl phosphate intercalated with tetrahydrofuran $\text{VOPO}_4\cdot(\text{CH}_2)_4\text{O}$ is tetragonal, space group $P4/n$; $a = 6.208$, $c = 8.930 \text{ \AA}$; $Z = 2$, $D_x = 2.51 \text{ g cm}^{-3}$. The way guest thf molecules are anchored to the host VOPO_4 layer is

¹Supplementary data for this paper are available from the IUCr electronic archives (Reference: AV0032). Services for accessing these data are described at the back of the journal.

illustrated in detail in Fig. 3, where one can see the two possible orientations of thf molecules, attached to the lower and upper host layer *via* the thf oxygen. The size of the guest species and the distances between active sites are in favourable mutual relation as well as the host–guest and guest–guest interactions resulting in the regular monolayer arrangement of the thf molecules in the interlayer space and regular layer stacking. Interlayer crystal packing and layer stacking in thf-VOPO₄ is illustrated in Fig. 7 (side and upper view).

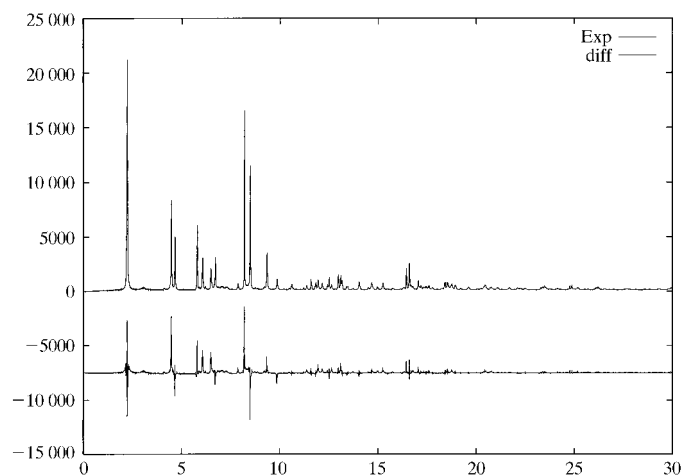


Figure 6
Bond-restrained Rietveld refinement DEG-VOPO₄. The upper curve illustrates the observed data, while the lower curve is the difference between observed and calculated data.

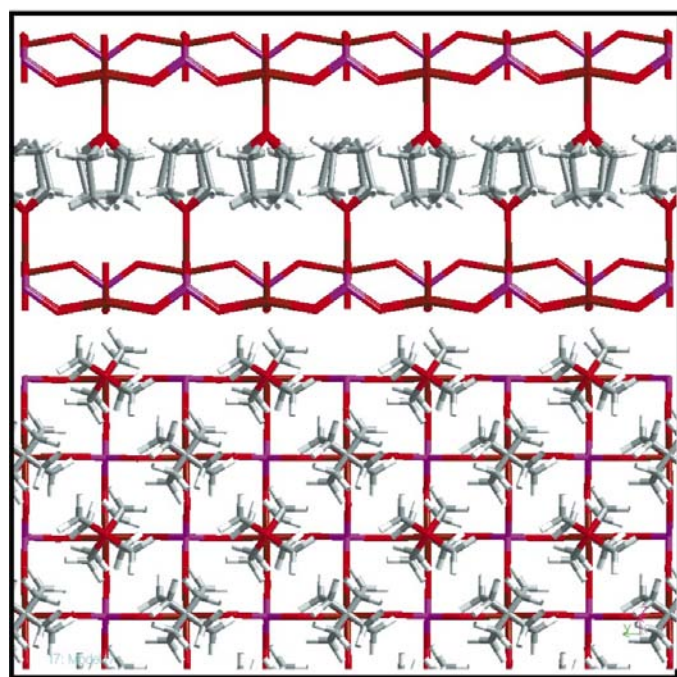


Figure 7
The crystal packing of the intercalate thf-VOPO₄. Upper figure shows the interlayer arrangement, lower figure shows the side view and the space filling.

4.2. Structure of DEG-VOPO₄

The structure of DEG-VOPO₄ is tetragonal, space group $P4/n$, $a = 6.223$, $c = 11.417$ Å, $Z = 2$, density $D_x = 2.66$ g cm⁻³. Fig. 4 illustrates the anchoring of the DEG molecule to the V atom *via* its central O atom, where one can see two possible orientations of DEG molecules, with occupancy 0.5. It is clear from a comparison of Figs. 3 and 4 that the DEG molecule is too large compared with the distances between the active sites (*i.e.* V–V distances). As a result of this, the guest molecules are arranged in two layers in the interlayer space of the host structure.

Crystal packing in DEG-VOPO₄ is illustrated in Fig. 8, upper figure – side view, lower figure – view perpendicular to the layers, where the yellow and pink colour denotes the upper and lower DEG layer in the VOPO₄ interlayer space. In spite of the bilayer arrangement of the guest molecules, the layer stacking in this structure is regular, without any displacement disorder, which is usually observed in intercalates with a bilayer arrangement of guests. Examples of displacement disorder in layer stacking in intercalates with a bilayer arrangement of guests are vanadyl phosphate intercalated with ethanol (Čapková, Beneš *et al.*, 1998), and with 1-alkanols (Čapková *et al.*, 2000) and in α -zirconium phosphate intercalated with ethanol (Čapková, Janeba *et al.*, 1998). There are two main reasons for the regular layer stacking of the DEG-VOPO₄ structure:

a regular arrangement of the guest molecules with respect to the host layer and

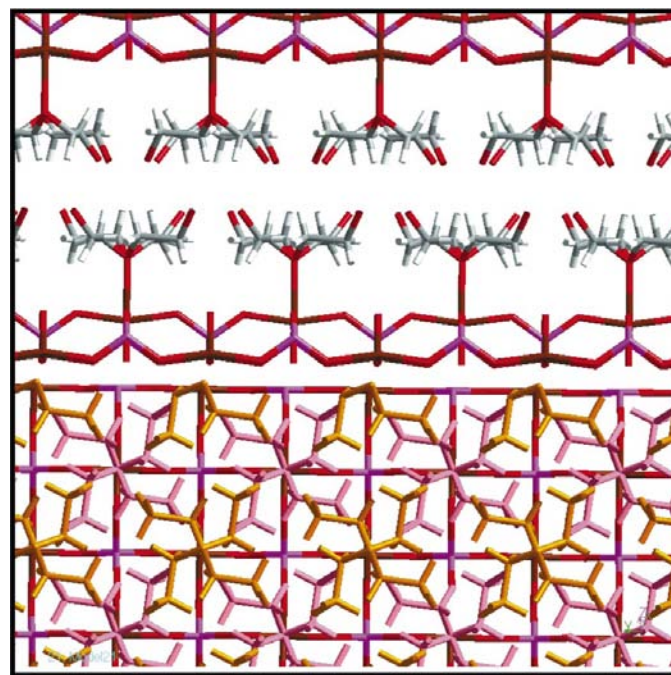


Figure 8
The crystal packing of the intercalate DEG-VOPO₄. Upper figure shows the interlayer arrangement, lower figure shows the side view and the space filling. For clarity the DEG molecules in the upper guest layer are yellow and in the lower guest layer the DEG molecules are pink.

the strong mutual guest–guest interactions between the DEG molecules in the lower and upper guest layers, which restrict the guest layers to attain well defined positions. These two conditions are not fulfilled in the case of alkanol molecules. Ethanol molecules are too small in comparison with the space between the active sites and this allows quite a high degree of positional and orientational disorder in their arrangement and orientation, and consequently in the stacking of the host layers.

5. Conclusions

The present results show that molecular simulations are a very useful complementary tool in the structure determination of intercalates, as these structures exhibit two main special features, which may obstruct the structure analysis based on powder diffraction data alone. First of all there may be a certain degree of disorder in the interlayer space (in the present case two possible orientations of guest molecules). The second important feature is that the organic molecules intercalated into the inorganic host structure do not completely obey the rules for crystal packing of molecular crystals, as they are forced by the crystal field of the host structure to arrange themselves according to the arrangement of the active sites on the host layer. This competition between the host–guest and guest–guest interaction results in an interlayer density which is usually higher than in normal molecular crystals. As a result of these two unfavourable circumstances, electron-density maps obtained from diffraction data are smooth and difficult to analyse.

The results of the present structure analysis also show the effect of geometrical factors and interaction energy characteristics on the arrangement of guest molecules and layer stacking in intercalates. In the case of thf–VOPO₄ the distance between the active sites on the host layer, *i.e.* the distance between the V atoms (8.93 Å), allows the regular monolayer arrangement of thf molecules in the interlayer space. On the other hand, in the case of DEG–VOPO₄ the size of DEG molecules is too large in comparison with the distance of the active sites. Consequently, the guest molecules create a bilayer arrangement in the interlayer space, as illustrated in Fig. 8, where one can see the partial overlap of upper and lower guest

layers and where one can also see the mutual relationship between the size of DEG and the V–V distance.

The authors would like to thank Dr A. N. Fitch from BM16 at ESRF in Grenoble for his help during the high-resolution powder diffraction measurements. This work was supported by the Grant Agency of Charles University (grant No: 37/97/B) and by the Ministry of Education of Czech Republic (project MSM 113200001).

References

- Ahtee, M., Nurmela, M., Suortti, P. & Järvinen, M. (1989). *J. Appl. Cryst.* **22**, 261–268.
- Beneš, L., Melánová, K., Zima, V., Kalousová, J. & Votinský, J. (1997). *Inorg. Chem.* **36**, 2850–2854.
- Burchart, E. de Vos (1992). Ph.D. Thesis. Technische Universiteit Delft, The Netherlands.
- Čapková, P., Beneš, L., Melánová, K. & Schenk, H. (1998). *J. Appl. Cryst.* **31**, 845–850.
- Čapková, P., Janeba, D., Beneš, L., Melánová, K. & Schenk, H. (1998). *J. Mol. Model.* **4**, 150–157.
- Čapková, P., Melánová, K., Beneš, L. & Schenk, H. (2000). *J. Mol. Model.* **6**, 9–16.
- Chernyshev, V. V. & Schenk, H. (1998). *Z. Kristallogr.* **213**, 1–3.
- Clearfield, A. (1982). Editor. *Inorganic Ion Exchange Material*. Boca Raton, Florida: CRC Press, Inc.
- Costantino, U. (1981). *J. Inorg. Nucl. Chem.* **43**, 1895–1902.
- Fitch, A. N. (1996). *Materials Science Forum*, edited by R. J. Cernik, R. Delhez and E. J. Mittenmeijer, Vol. 228. Aedermannsdorf: Trans Tech Publications.
- Järvinen, M. (1993). *J. Appl. Cryst.* **26**, 525–531.
- Ladwig, G. (1965). *A. Anorg. Allg. Chem.* **338**, 266–270.
- Melánová, K., Beneš, L., Zima, V., Vahalova, R. & Kilian, M. (1999). *Chem. Mater.* **11**, 2173–2178.
- Molecular Simulations Inc. (1995). *Cerius²*, Release 2.0 Biosym/Molecular Simulations Inc., San Diego, USA.
- Ogawa, M. & Kuroda, K. (1995). *Chem. Rev.* **95**, 399–438.
- Rappé, A. K., Casewit, C. J., Colwell, K. S., Goddard III, W. A. & Skiff, W. M. (1992). *J. Am. Chem. Soc.* **114**, 10024–10035.
- Rappé, A. K. & Goddard III, W. A. (1991). *J. Phys. Chem.* **95**, 3358–3363.
- Tachez, M., Theobald, F., Bernard, J. & Hewat, A. W. (1982). *Rev. Chim. Mineral.* **19**, 292–300.
- Tietze, H. R. (1981). *Aust. J. Chem.* **34**, 2035–2038.
- Zlokazov, V. B. & Chernyshev, V. V. (1992). *J. Appl. Cryst.* **25**, 447–451.